

See discussions, stats, and author profiles for this publication at: <https://www.researchgate.net/publication/224012765>

# The ionization potential of Si<sub>2</sub>N and Si<sub>2</sub>O

ARTICLE *in* THE JOURNAL OF PHYSICAL CHEMISTRY A · JULY 2002

Impact Factor: 2.69 · DOI: 10.1021/jp020468j

---

CITATIONS

4

---

READS

45

4 AUTHORS, INCLUDING:



[James L Gole](#)

Georgia Institute of Technology

356 PUBLICATIONS 6,966 CITATIONS

SEE PROFILE



[David A Dixon](#)

University of Alabama

766 PUBLICATIONS 22,154 CITATIONS

SEE PROFILE



[Kirk A Peterson](#)

Washington State University

273 PUBLICATIONS 16,044 CITATIONS

SEE PROFILE

# The Ionization Potential of Si<sub>2</sub>N and Si<sub>2</sub>O<sup>†</sup>

S. J. Paukstis and J. L. Gole\*

*School of Physics, Georgia Institute of Technology, Atlanta, Georgia 30332-0430*

David A. Dixon

*William R. Wiley Environmental Molecular Sciences Laboratory, Pacific Northwest National Laboratory, P.O. Box 999, Richland, Washington 99352*

Kirk A. Peterson

*Department of Chemistry, Washington State University, Richland, Washington 99352, and William R. Wiley Environmental Molecular Sciences Laboratory, Pacific Northwest National Laboratory, P.O. Box 999, Richland, Washington 99352*

*Received: February 20, 2002; In Final Form: March 5, 2002*

One-color resonant and nonresonant ionization studies of Si<sub>2</sub>N and Si<sub>2</sub>O have been performed using a pulsed laser vaporization cluster source in conjunction with a time-of-flight mass spectrometer. The ionization potential of Si<sub>2</sub>N is established as less than 6.4 eV, while the ionization potential of Si<sub>2</sub>O is bracketed between 6.4 and 7.9 eV. The experimentally established ionization potential for Si<sub>2</sub>N is confirmed by detailed molecular electronic structure calculations which indicate an adiabatic as well as vertical ionization potential of  $6.2 \pm 0.05$  eV and a close similarity between neutral Si<sub>2</sub>N and ionic Si<sub>2</sub>N<sup>+</sup>. Similar detailed calculations lead to a best estimate of an adiabatic ionization energy of  $7.42 \pm 0.04$  eV and a vertical ionization energy of  $7.66 \pm 0.04$  eV for Si<sub>2</sub>O.

## Introduction

Although the molecular electronic structure of the silicon-based diatomics of carbon, nitrogen, oxygen, and fluorine have been well studied,<sup>1</sup> information on even the simplest polyatomic combination of these atoms is sparse. An important quantity whose establishment can contribute to the modeling of these systems is the ionization potential. Here we will consider the ionization potential of Si<sub>2</sub>N and set bounds on the energy required to ionize Si<sub>2</sub>O.

The first experimental study of Si<sub>2</sub>N, a mass spectroscopic analysis of silicon vaporized from a boron nitride Knudsen cell, predicted the ionization potential of Si<sub>2</sub>N to be  $9.4 \pm 0.3$  eV by the vanishing-current method.<sup>2</sup> Iraqi, Goldberg, and Schwarz<sup>3</sup> and later Goldberg et al.<sup>4</sup> conducted gas-phase neutralization–reionization mass spectrometry (NRMS) studies on Si<sub>2</sub>N, noting a stable Si<sub>2</sub>N and favorable Franck–Condon factors for ionization of the molecule. The later study, which combined an NRMS analysis of Si<sub>3</sub>N with a reasonable ab initio analysis of the energetics of the neutral Si<sub>2</sub>N molecule, its cation and anion, established a linear *D<sub>∞h</sub>* geometry to be the global minimum for the Si<sub>2</sub>N molecule. The adiabatic ionization energy for removal of an electron from the <sup>2</sup>Π<sub>g</sub> ground electronic state was predicted to be 6.2 eV. Further theory<sup>5</sup> confirmed the prediction of Goldberg et al.<sup>4</sup> that a cyclic *C<sub>2v</sub>* conformer lies only 4.5 kcal/mol higher in energy than the ground electronic state.

The prediction of an ionization potential less than 6.4 eV for Si<sub>2</sub>N has been called into question in conjunction with the most recent experimental investigation of this molecule by Brugh and

Morse.<sup>6</sup> Using one-color resonant ionization, they established experimentally that a linear centrosymmetric isomer of <sup>2</sup>Π<sub>g</sub> symmetry does exist in the gas phase, and that the IP of Si<sub>2</sub>N is less than 8.51 eV. The 34314 cm<sup>−1</sup> band of a <sup>2</sup>Σ<sub>u</sub><sup>+</sup>–<sup>2</sup>Π<sub>g</sub> transition was rotationally resolved, and molecular constants were derived for both the ground (<sup>2</sup>Π<sub>g</sub>) and excited (<sup>2</sup>Σ<sub>u</sub><sup>+</sup>) states. They obtained a low resolution vibronic spectrum over the range 33600–36000 cm<sup>−1</sup>, but were unable to fit the observed bands to a progression. This limitation was attributed to the possibility that both the linear and cyclic symmetric isomers were present in their system and represented in the spectrum. Further, given that the determined Si–N bond length changed in the transition from ground (1.6395 Å) to excited state (1.6343 Å) by only +0.0052 Å, they suggested that the transition corresponded to the promotion of an electron from a ground-state nonbonding (2σ<sub>u</sub>) to a nonbonding (1π<sub>g</sub>) orbital.

On the basis of the nonbonding character of the (1π<sub>g</sub>) orbital, Brugh and Morse concluded that the IP of Si<sub>2</sub>N would not significantly differ from the IP of atomic silicon, 8.1 eV,<sup>7</sup> because the electron removed is “mainly [Si 3p] nonbonding in character”. Certainly the conclusions of Brugh and Morse add controversy to the establishment of a correct value for the Si<sub>2</sub>N ionization potential. Even if the cyclic isomer of Si<sub>2</sub>N is ionized in their study, a lower bound consistent with previous estimates of the Si<sub>2</sub>N ionization potential should not exceed 6.6 eV, a far cry from the ionization potential of atomic silicon. Thus, this system bears further investigation.

The first theoretical study of Si<sub>2</sub>O was published in 1989 by DeKock, Yates, and Schaefer,<sup>8</sup> but they restricted their ab initio SCF calculations to the symmetric and antisymmetric linear states of the molecule. Boldyrev and Simons<sup>9</sup> later considered

<sup>†</sup> Part of the special issue “Donald Setser Festschrift”.

\* Corresponding author.

these states as well as the bent symmetric isomer. Their calculations showed the global minimum to be the bent singlet  $C_{2v}$  ( $^1A_1$ ) Si–O–Si structure, with all triplet states lying at least 17 kcal/mol higher in energy. Using the results predicted by these researchers, Iraqi, Goldberg, and Schwarz<sup>3</sup> claimed to show the first experimental evidence in support of triangular Si<sub>2</sub>O in their 1993 NRMS study. In 1994, Boldyrev et al.,<sup>10</sup> using several basis sets and methods, estimated the vertical IP of the cyclic form of Si<sub>2</sub>O to be  $7.5 \pm 0.2$  eV. However, there appear to be no experimental confirmations of this value.

## Experimental Section

The Si<sub>2</sub>N and Si<sub>2</sub>O molecules were produced in a pulsed laser vaporization cluster source. External to the vacuum chamber, the carrier gas (helium) and the reactant gases NO<sub>2</sub>, N<sub>2</sub>O, and CO<sub>2</sub> were combined in a commercially available gas proportioner system (Air Products 150 mm stainless steel) and fed through nalgene tubing into the back of the pulsed valve assembly. Simultaneously, the fundamental output of a Nd:YAG laser ( $\lambda = 1.06 \mu\text{m}$ ) was focused onto a rotating and translating silicon rod. A pulsed valve (Lasertechnics model 201) provided a high-pressure burst of the mixed carrier/reactant gas, which entrained the material ablated from the rod, and directed the resulting clusters toward the end of a nozzle channel. Upon exiting the nozzle the mixture underwent supersonic expansion (into vacuum). The resulting molecular beam was skimmed by a 4 mm diameter skimmer as it passed into a time-of-flight chamber. The time-of-flight mass spectrometer employed for these studies has been described previously.<sup>11</sup>

The gases N<sub>2</sub>O and NO<sub>2</sub> were used to form Si<sub>2</sub>N as opposed to pure nitrogen, N<sub>2</sub>.<sup>6,12</sup> While it might be argued that the presence of oxygen complicates product formation, N<sub>2</sub> with its triple bond has a dissociation energy of 9.8 eV,<sup>13</sup> as opposed to, for example, an N–NO bond energy<sup>14</sup> of 4.93 eV. Thus N<sub>2</sub>O much more easily gives up a nitrogen for the formation of Si<sub>2</sub>N and, in fact, the intensities observed for Si<sub>2</sub>N in this study<sup>15</sup> considerably exceed those reported by Brugh.<sup>12,16</sup> The mass selected spectroscopy done in this study also ensures that both Si<sub>2</sub>N and Si<sub>2</sub>O product formation is monitored as the system is also sensitive to complex formation with these two molecules via the observation of metastable peaks in the TOF spectrum.<sup>17</sup>

One-color nonresonant ionization was accomplished using excimer laser (Lambda-Physik EMG 103) radiation at 157 (F<sub>2</sub>), 193 (ArF), and 248 (KrF) nm. “High flux”, which corresponds to a fluence well in excess of 50 mJ/cm<sup>2</sup>, will be used to describe conditions for nonresonant multiphoton excitation with ArF or KrF excimer photons simultaneously exciting sample Si<sub>2</sub>N or Si<sub>2</sub>O molecules under the alignment conditions of the experiment. “Low flux” will describe conditions for the ArF and F<sub>2</sub> lasers for which the fluence was less than 5 mJ/cm<sup>2</sup> incident upon the Si<sub>2</sub>N or Si<sub>2</sub>O molecular beams. For ArF the resultant ion intensity varied linearly with laser power. Two-color resonant ionization for Si<sub>2</sub>N was accomplished with a Nd:YAG pumped dye laser operating in the R590, P597, and R610 ranges and supplying light which was frequency doubled by a KDP crystal. The resulting tunable UV light provided energy for ionization via one-color resonant intermediate excitation and produced results in agreement with Brugh and Morse.<sup>7</sup>

Ions were detected by a microchannel plate detector (Galileo Electrooptics model FTD-2003) at the top of a time-of-flight tube. The resulting signal was amplified by a 20 dB video amplifier (Comlinear CLC100) before being sent to the appropriate data acquisition device. For nonresonant results, a

transient digitizer/signal averager combination (DSP Technology 2101) was used to rapidly sum ion signals over a variable time window.

## Calculations

Calculations on the ground state of Si<sub>2</sub>N and Si<sub>2</sub>N<sup>+</sup> were carried out at the coupled cluster level of theory with single and double excitations and a perturbative correction for the triple excitations [CCSD(T)].<sup>18</sup> The initial energetics were calculated within the frozen core (FC) approximation in which the 10 inner shell electrons (1s<sup>2</sup>2s<sup>2</sup>2p<sup>6</sup>) on each silicon atom and the two inner shell 1s<sup>2</sup> electrons were excluded from the correlation treatment. When combined with large basis sets, the CCSD(T)(FC) level of theory is capable of recovering a significant fraction of the valence correlation energy. There are currently three widely used CCSD(T) approaches for handling open shell systems.<sup>18,19</sup> The calculations on the open shell ground state of Si<sub>2</sub>N (linear,  $^2\Pi_g$ ), Si<sub>2</sub>O<sup>+</sup> (linear,  $^2\Pi_g$ ), and Si<sub>2</sub>O<sup>+</sup> (bent,  $^2A_1$ ) were done with ROHF orbitals, but with the spin constraint relaxed in the coupled cluster portion of the calculation. Energies obtained from this hybrid procedure are denoted R/UCCSD(T). The Si<sub>2</sub>N<sup>+</sup> ion and Si<sub>2</sub>O are closed shell, so there is no issue with the form of the CCSD(T) calculations. All calculations were performed with the MOLPRO-2000<sup>20</sup> program on Silicon Graphics PowerChallenge compute servers.

All calculations were performed with the correlation consistent (cc-pVnZ) basis sets.<sup>21</sup> These sequences of basis sets have been extensively demonstrated to provide reliable thermochemical and structural properties, with rare exceptions.<sup>22</sup> Only the spherical components (i.e., 5-d, 7-f, 9-g, etc.) of the Cartesian basis functions were used. The geometries were optimized at the CCSD(T) level with the cc-pVDZ and cc-pVTZ basis sets. Energies were obtained at the CCSD(T)/cc-pVQZ level with the CCSD(T)/cc-pVTZ optimized geometry in order to extrapolate to the complete basis set limit. To estimate energies at the complete basis set (CBS) limit, we used a mixed exponential/Gaussian function of the form:

$$E(n) = A_{\text{CBS}} + B \cdot \exp[-(n-1)] + C \cdot \exp[-(n-1)^2] \quad (1)$$

where  $n = 2$  (DZ), 3 (TZ), etc., first proposed by Peterson et al.<sup>23</sup> We denote this as CBS(aDTQ/mix). In the studies of Feller and Peterson,<sup>22e,f</sup> the mixed expression produced the smallest mean absolute deviation with respect to experiment by a small measure as compared to other extrapolation methods such as the simple exponential.

Having estimated energies at the CCSD(T)(FC)/CBS level of theory, we then include a number of additional corrections to account for core-valence and molecular scalar relativistic effects. Core-valence corrections to the ionization energy were obtained from fully correlated CCSD(T) calculations (excluding only the 1s<sup>2</sup> electrons on Si) with the cc-pCVTZ basis set<sup>24</sup> at the CCSD(T)/cc-pVTZ geometry. We evaluate the scalar relativistic correction using configuration interaction wave functions with single and double excitations (CISD/cc-pVTZ)<sup>25</sup> at the CCSD(T)/cc-pVTZ geometry. Specifically, the scalar relativistic energy lowering is defined to be the sum of the expectation values of the 1-electron Darwin and mass–velocity terms in the Breit-Pauli Hamiltonian. Zero-point vibrational energies are also evaluated. The frequencies for the ion Si<sub>2</sub>N<sup>+</sup> were calculated at the CCSD(T)/cc-pVDZ level. The frequencies for Si<sub>2</sub>N were taken from Ornellas and Iwata who obtained these values at the CCSD(T)/cc-pVTZ level.

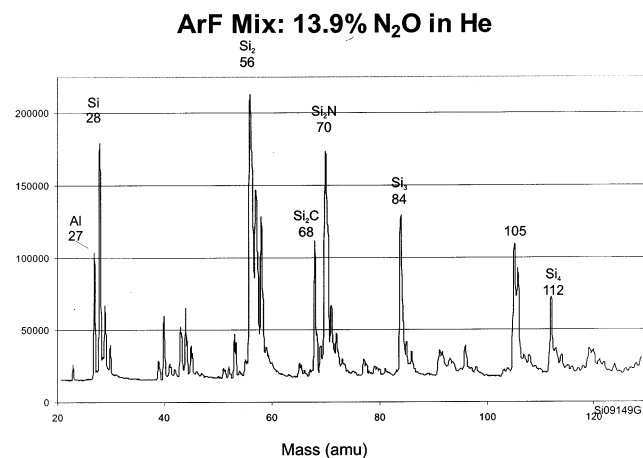


**Figure 1.** Time-of-flight mass spectrum for Si<sub>x</sub> + He + N<sub>2</sub>O expansion after multiphoton excitation (simultaneous “nonresonant” two-photon) with an ArF excimer laser (12.8 eV).

## Results

**Si<sub>2</sub>N and Si<sub>2</sub>O Ionization Potential Bounds—Non-Resonant Ionization.** “Si<sub>2</sub>N”. Silicon atoms and molecules were produced in supersonic expansion using pulsed laser vaporization as the resulting product formation from both pure helium and oxidant-seeded expansions was studied mass spectrometrically. Mass spectral data devoid of metastable peaks<sup>17</sup> for these nonresonant experiments was collected using the DSP Technology PSP system (equipped with a CAMAC crate) as the analysis was accomplished using the “Pspasil” program and a PC spreadsheet program (Microsoft Excel 97). A custom-designed visual basic macro entitled “psp” was used from within Excel to convert the data for examination. To form and study Si<sub>2</sub>N, a source of nitrogen was necessary. This was provided to the system by mixing a small percentage (1–15%) of N<sub>2</sub>O or NO<sub>2</sub> (typically 17%) into a helium carrier gas. To form Si<sub>2</sub>O, the oxygen sources were N<sub>2</sub>O, NO<sub>2</sub>, and CO<sub>2</sub>. Si<sub>2</sub>O appears to be formed less efficiently than Si<sub>2</sub>N.

A comparison of the mass spectra obtained under nonresonant ArF multiphoton excitation both with a helium-only expansion and with N<sub>2</sub>O (Figure 1) reveals that AlO, SiO, and Si<sub>2</sub>N all increase when N<sub>2</sub>O is added to the system. AlO is formed due to the laser vaporization of aluminum from the walls of the expansion nozzle channel.<sup>17</sup> This result suggests that N<sub>2</sub>O dissociates in the laser vaporization plasma, with the resulting components reacting with aluminum or silicon-based constituents in the system. The data in Figure 1 were obtained when all the conditions for multiphoton ArF (6.4 eV) excitation were met, the available energy corresponding at least to a two-photon absorption at 12.8 eV. The spectra depicted in Figure 1 were obtained with ~14% N<sub>2</sub>O mixed into the helium carrier expansion gas. That a signal corresponding to mass 70 is observed implies that either the IP of the ionizing molecule in question is less than 12.8 eV or the molecule has eigenstates resonant with the ArF photon energy (51850 cm<sup>-1</sup> = 6.4 eV).

The data in Figure 2 were obtained with multiphoton excitation from a KrF laser (≥10 eV). Large silicon atom (IP = 8.1 eV<sup>7</sup>) and Si<sub>2</sub>C (IP = 9.4 eV<sup>26</sup>) ion signals are observed in this scan. Further experiments<sup>27</sup> to excite resonant two-photon spectra from Si<sub>2</sub>C (as opposed to SiC<sub>2</sub>) indicate that neither Si or Si<sub>2</sub>C have energy levels readily accessed with KrF excitation. A photon energy of 5 eV is insufficient to ionize these constituents, consistent with the fact that they are formed via a nonresonant multiphoton ionization process. The dramatic

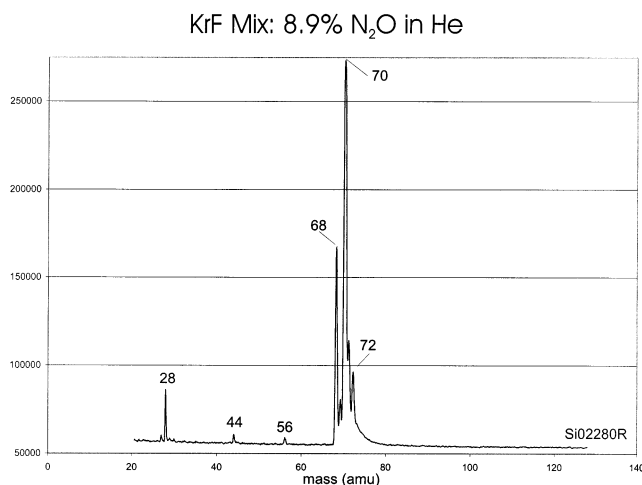


**Figure 2.** Time-of-flight mass spectrum for Si<sub>x</sub> + He + N<sub>2</sub>O expansion after multiphoton excitation (simultaneous “nonresonant” two-photon) with a KrF excimer laser (10 eV).

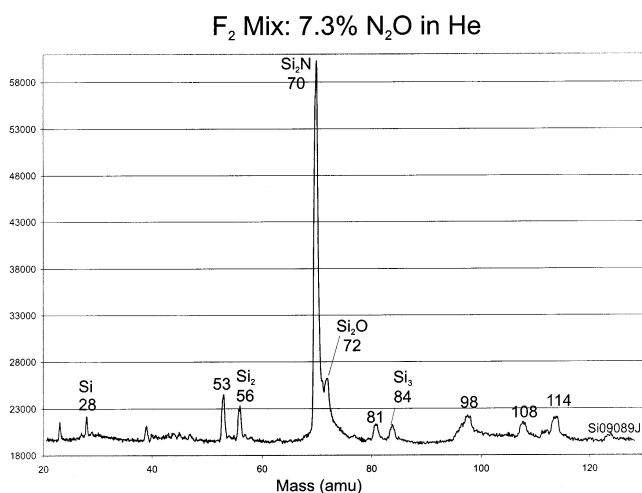


**Figure 3.** Time-of-flight mass spectrum for Si<sub>x</sub> + He + N<sub>2</sub>O expansion after excitation with an F<sub>2</sub> laser at 7.9 eV.

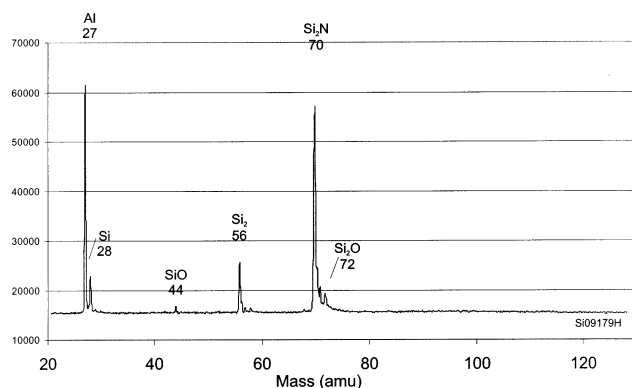
increase in the mass 70 signal from the ArF MPI mass spectrum (Figure 1) to the KrF MPI mass spectrum (Figure 2) suggests the resonance excitation of the molecule or at least a portion of the molecules corresponding to mass 70. The IP of the molecules giving rise to the mass 70 peak is most likely less than the energy available for two-photon ionization, ( $2h\nu = 2 \times 5.0$  eV) 10.0 eV, consistent with both Si<sub>2</sub>N and Al<sub>2</sub>O.

It is important to note that the Al<sub>2</sub>O molecule, which might be formed due to aluminum vaporization from the walls of the expansion nozzle channel, can contribute to the mass 70 signal observed in the ArF and KrF scans. The IP of Al<sub>2</sub>O has been established at  $8.5 \pm 0.2$  eV.<sup>28</sup> Thus, while Al<sub>2</sub>O<sup>+</sup> may be present in the ArF and KrF MPI scans, it does not account for any portion of the observed mass 70 signal when ionization energies are less than 8.5 eV. Further, the Al<sub>2</sub>O resonant electronic spectrum can be readily distinguished from that of Si<sub>2</sub>N.<sup>15,27,29</sup> As we compare the mass 70 signal strength in Figure 3, obtained with fluorine excimer excitation (= 5 mJ/cm<sup>2</sup>), we observe a large drop in signal from the multiphoton ArF and KrF scans. This drop roughly corresponds to a loss of approximately 2/3 of the counts obtained above 7.9 eV, suggesting that Al<sub>2</sub>O indeed contributes to the mass 70 signal in simultaneous multiphoton ArF and KrF excitation.



**TABLE 1: Summary of Ionization Potential Data on Si<sub>2</sub>N**

ionization scheme	energy observed	results
ArF + ArF	12.8 eV	Large non-resonant 70 signal
KrF + KrF	10.0 eV	Large nonresonant mass 70 signal
	9.4 eV	Si <sub>2</sub> N IP predicted by Zmbov, Margrave <sup>2</sup>
PDL + KrF	9.26 eV	Resonant Si <sub>2</sub> N signal observed, R2PI spectrum taken <sup>15</sup>
PDL + PDL	8.52 eV	Resonant Si <sub>2</sub> N signal observed in agreement with Brugh and Morse, <sup>6</sup> R2PI spectrum taken <sup>15</sup>
PDL + N <sub>2</sub>	7.94 eV	No Si <sub>2</sub> N resonant signal observed, N <sub>2</sub> laser photon flux too low
F <sub>2</sub>	7.90 eV	Nonresonant Si <sub>2</sub> N signal
ArF	6.40 eV	Nonresonant Si <sub>2</sub> N signal
	6.20 eV	Si <sub>2</sub> N IP predicted by Goldberg et al. <sup>4</sup>

**ArF Mix: 6.7% N<sub>2</sub>O in He****Figure 4.** Time-of-flight mass spectrum for Si<sub>x</sub> + He + N<sub>2</sub>O expansion after excitation with an ArF laser at 6.4 eV.

The single photon energy associated with fluorine excimer laser excitation is 7.9 eV. The main feature observed in Figure 3 corresponds to an Si<sub>2</sub>N peak implying that either Si<sub>2</sub>N has eigenstates resonant with the F<sub>2</sub> photon energy (63709 cm<sup>-1</sup>), or its ionization potential lies below 7.9 eV. All other mass signals are smaller than the Si<sub>2</sub>N peak by at least a factor of 6.

When the system was operated at low power = 5 mJ/cm<sup>2</sup> (excitation from an ArF excimer laser), the mass spectrum depicted in Figure 4 was obtained. Here the ionizing energy, dominantly 6.4 eV, is sufficient to excite aluminum (IP 5.98 eV<sup>30</sup>) whose mass spectral signal is almost six times that of silicon (IP = 8.1 eV<sup>7</sup>). The trace Si, SiO, and Si<sub>2</sub> signals most likely result from small contributions from two-photon non-resonant events. However, regardless of the reduction in power, the Si<sub>2</sub>N signal remains prominent and is approximately linear in laser power down to the lowest fluences producing a mass 70 signal in the scan of Figure 4. This suggests that the Si<sub>2</sub>N molecule is undergoing single-photon ionization and the IP must be less than 6.4 eV.

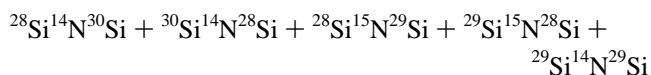
With an accelerating field of 394 V/cm, the appearance potential is lowered from the true IP of the molecule in question by approximately 121.5 cm<sup>-1</sup>, or about 0.015 eV.<sup>11</sup> This means that the nonresonant ionization potential results obtained here were, within our limits of resolution, unaffected by the electric field. This result is in agreement with previous studies.<sup>11</sup> Very similar results as a function of excimer photon energy and photon flux are obtained when NO<sub>2</sub> is seeded into an Si<sub>x</sub>/He supersonic expansion, suggesting that the nitrogen source emanates from the complete dissociation of NO<sub>2</sub>. A summary of results is presented in Table 1.

“Si<sub>2</sub>O”. Si<sub>2</sub>O proved much more difficult to form than Si<sub>2</sub>N, and its nonresonant signal is much smaller than the dominant Si<sub>2</sub>N peaks. An additional complication arises from the fact that Si<sub>2</sub>N has both mass 70 and mass 72 isotopes. The data in Table 2 imply that part of the mass 72 signal may be attributable to

**TABLE 2: Isotopes of Silicon and Nitrogen**

silicon abundance		nitrogen abundance	
mass (amu)	(%)	mass (amu)	(%)
28	92.23	14	99.64
29	4.67	15	0.36
30	3.10		

a combination of the “heavier” silicon and nitrogen isotopic abundances. Possible combinations of isotopes that form mass 72 are:



with isotope abundances of

$$2.849\% + 2.849\% + 0.016\% + 0.016\% + 0.217\%$$

for a total mass 72 abundance of 5.947% of the total available Si<sub>2</sub>N.

Analysis of nonresonant spectra for mass 72 will rely heavily upon the proportion of mass 70 (<sup>70</sup>Si<sub>2</sub>N and Al<sub>2</sub>O) to mass 72 (<sup>72</sup>Si<sub>2</sub>N and Si<sub>2</sub>O) observed. The lower the ratio, the more mass 72 is being observed. Because the ionization potential of Si<sub>2</sub>N is less than that predicted<sup>4,10</sup> for Si<sub>2</sub>O, it was anticipated that proportionately more Si<sub>2</sub>N would ionize than Si<sub>2</sub>O. (The ionization efficiencies of the respective molecules may modify this effect somewhat). The natural isotopic ratio of mass 70 to mass 72 for Si<sub>2</sub>N alone is 84.76%:5.94%, or 14.25:1. In the present study, the size of the Si<sub>2</sub>N (mass 70) peak is not within itself fundamental to the conclusions reached here. *Rather, it is the mass 70 to mass 72 ratio from which our conclusions will be drawn.*

To form and study Si<sub>2</sub>O, it was necessary to provide a source of oxygen. This was provided to the system by mixing a small percentage (6.7–13.9%) of N<sub>2</sub>O, NO<sub>2</sub> (typically 17%), or CO<sub>2</sub> (typically 6.25%) into the helium carrier gas. A comparison of the mass spectra obtained under ArF multiphoton (dominantly two photon) excitation both with helium only and with N<sub>2</sub>O (Figure 1) reveals, through the examination of the Si<sub>2</sub>O peak (mass 72), that there is a decrease in the ratio of mass 70 to mass 72 as the reactant N<sub>2</sub>O is added. This ratio is 8.72:1 for helium alone and 5.85:1 for helium + N<sub>2</sub>O. This indicates that free oxygen contributes to the Si<sub>2</sub>O (mass 72) signal, and that the ionization potential of Si<sub>2</sub>O is less than 12.8 eV.

Figure 2 depicts a mass spectral scan taken under KrF high flux conditions with 8.9% N<sub>2</sub>O in helium. The ratio of mass 70–mass 72 in this scan is 5.35:1. Preliminary molecular electronic structure calculations of the excited states of bent singlet (C<sub>2v</sub>) Si–O–Si suggest the possibility that ionization may proceed through resonance with an intermediate state. The results depicted in Figure 2 demonstrate that the IP of Si<sub>2</sub>O must be less than the available energy for two-photon ionization, 10 eV.

**TABLE 3: Mass 70–Mass 72 Peak Ratios for Various Reactant Gases and One- or Two-Photon Ionization**

reactant mixture	laser combination	Ratio Mass 70–Mass 72 <sup>a</sup>
Si <sub>x</sub> + He	ArF + ArF	8.5–8.7:1
Si <sub>x</sub> + He + N <sub>2</sub> O	ArF + ArF	5.5:1
	KrF + KrF	5.35:1
	F <sub>2</sub>	6.26:1
	ArF	11.2:1
Si <sub>x</sub> + He + NO <sub>2</sub>	ArF + ArF	~4.5:1
	KrF + KrF	5.36:1
	ArF	7.24:1
Si <sub>x</sub> + He + CO <sub>2</sub>	ArF + ArF	6.0:1
	ArF	7.29:1
	ArF	7.29:1

<sup>a</sup> Natural abundance ratio for Si<sub>2</sub>N = 14.25:1.

When the excimer gas mix is changed to a fluorine (F<sub>2</sub>) mix, with each ionizing photon having an energy of 7.9 eV, the mass spectrum depicted in Figure 3 is obtained. The ratio of mass 70 to mass 72 here is 6.26:1. This reveals approximately 26% more Si<sub>2</sub>O production than when helium was used as the sole carrier gas (~8.5:1). This indicates the presence of Si<sub>2</sub>O at concentration levels considerably above background, and thus that the IP of Si<sub>2</sub>O is less than 7.9 eV.

The results obtained using an ArF excimer mix at low flux are depicted in Figure 4, the mass 70–mass 72 ratio increased 32% above the ArF high flux helium-only ratio (~8.5:1) to 11.2:1. This indicates that the mass 72 signal has dropped significantly with respect to the mass 70 signal, which in turn reveals that at least some of the Si<sub>2</sub>O molecules which were ionized by 7.9 eV photons were not ionized by 6.4 eV photons. Therefore, it seems that the ionization potential of Si<sub>2</sub>O is above 6.4 eV.

The pattern of a jump in the mass 70–mass 72 ratio was repeated for NO<sub>2</sub> and CO<sub>2</sub> reactant gases (Table 3). Based on these results, the ionization potential of Si<sub>2</sub>O is bracketed between 6.4 and 7.9 eV in agreement with the calculations of Boldyrev and Simons.<sup>9</sup>

The molecular orbital structure of ground state (cyclic) Si<sub>2</sub>O (see following) is the same as that for cyclic Si<sub>2</sub>N with one additional electron located in the highest occupied molecular orbital. This orbital was predicted to be of antibonding Si•N character and bonding Si•Si character. At present, however, no theoretical or experimental studies had been published predicting the ionization potential of cyclic Si<sub>2</sub>N. If this value were known, it could be established whether the electron is removed from the bonding Si•Si framework (if IP cyclic Si<sub>2</sub>O > IP cyclic Si<sub>2</sub>N) or from the antibonding Si•N framework (IP cyclic Si<sub>2</sub>O > IP cyclic Si<sub>2</sub>N).

**Calculated Si<sub>2</sub>N Ionization Potential.** The optimized geometry at the CCSD(T)/cc-pVTZ level for Si<sub>2</sub>N has an Si–N bond length of 1.646 Å and for Si<sub>2</sub>N<sup>+</sup>, the Si–N bond distance is 1.629 Å. The valence electronic adiabatic ionization energy (IE) is 6.22 eV at the complete basis set limit. The vertical IE at the CCSD(T)/cc-pVQZ level is 6.22 eV as compared to an adiabatic IE of 6.20 eV at this level. The core valence correction is negligible and the relativistic correction lowers the IE by 0.01 eV. The zero-point energy difference raises the IE by 0.02 eV. This leads to a best estimate of the adiabatic ionization energy of 6.23 ± 0.04 eV with the vertical IE 0.02 eV higher at 6.25 ± 0.04 eV. The error bars are conservatively estimated from potential errors in the zero-point energy, basis set extrapolation procedure, and missing higher order correlation energy corrections.

**Calculated Si<sub>2</sub>O Ionization Potential.** The optimized geometry at the CCSD(T)/cc-pVTZ level for Si<sub>2</sub>O is bent with an

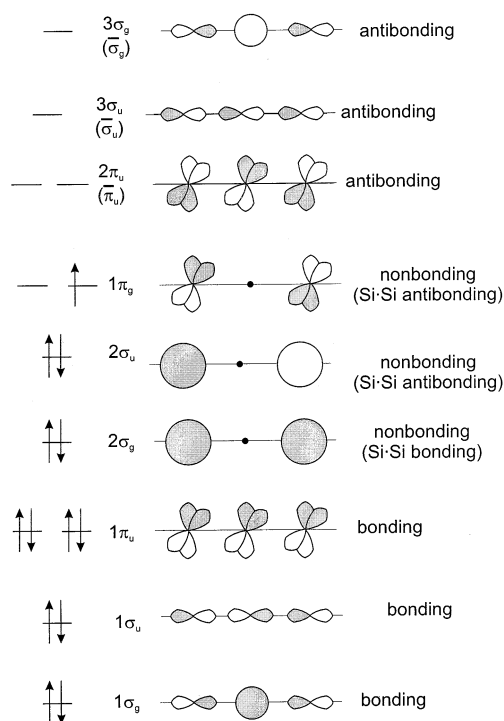


**Figure 5.** Molecular orbital diagram for linear Si–N–Si (BA<sub>2</sub>) showing appropriate combinations of atomic basis functions. Note that the ordering of the (2σ<sub>g</sub>) and (1π<sub>u</sub>) orbitals is transposed when increased interaction with the central nitrogen and s-p hybridization is considered. See text for discussion.

Si–O bond length of 1.718 Å and ∠SiOSi = 85.98°. The optimal geometry for Si<sub>2</sub>O<sup>+</sup> is bent with an Si–O bond length of 1.678 Å and ∠SiOSi = 99.37°. The bent structure for Si<sub>2</sub>O<sup>+</sup> only becomes more stable than the linear at the CCSD(T)/cc-pVQZ level. The linear structure for Si<sub>2</sub>O<sup>+</sup> (isoelectronic with Si<sub>2</sub>N) has an Si–O bond distance of 1.645 Å and is 0.83 kcal/mol higher in energy than the bent structure at the complete basis set limit for the valence electronic energy. The valence electronic adiabatic ionization energy (IE) is 7.44 eV at the complete basis set limit. The vertical IE at the CCSD(T)/cc-pVQZ level is 7.63 eV as compared to an adiabatic IE of 7.39 eV at this level. The core valence correction is negligible and the relativistic correction lowers the IE by 0.01 eV. The zero-point energy difference lowers the IE by 0.01 eV. This leads to a best estimate of the adiabatic ionization energy of 7.42 ± 0.04 eV with the vertical IE eV higher at 7.66 ± 0.04 eV.

## Discussion

**Simple Molecular Orbital Considerations.** Linear (*D<sub>∞h</sub>*) Molecular Orbital Configurations. We have constructed a schematic MO diagram to consider the nonresonant and resonant ionization of the Si<sub>2</sub>N molecule. Brugh and Morse<sup>6</sup> have simply stated that the molecular orbital configuration for Si<sub>2</sub>N is (1σ<sub>g</sub><sup>2</sup>1σ<sub>u</sub><sup>2</sup>1π<sub>u</sub><sup>4</sup>2σ<sub>g</sub><sup>2</sup>2σ<sub>u</sub><sup>2</sup>1π<sub>g</sub><sup>1</sup>). The most striking feature of the molecular orbital diagram which Brugh and Morse present is that the (nitrogen) 2s electrons are assumed to be “core-like” and nonbonding in character.

A modified molecular orbital diagram, constructed to give the same MO configuration as suggested by Brugh and Morse, is presented in Figure 5. This modified configuration, however, makes the assumption that, although the electronegativity of nitrogen is greater than that of silicon, electrons in the nitrogen 2s orbital are not so tightly bound as to not interact with the silicon 3s orbitals.

The molecular orbital scheme reported by Brugh and Morse<sup>6</sup> must also be modified to account for the  $\text{Si}_2\text{N}$  MO configuration predicted by previous theoretical studies.<sup>4,5</sup> Goldberg and co-workers<sup>4</sup> predicted the linear  $D_{\infty h}$  symmetry species ( $^2\Pi_g$ ;  $1\sigma_g^2 1\sigma_u^2 2\sigma_g^2 1\pi_u^4 2\sigma_u^2 1\pi_g^1$ ) configuration of  $\text{Si}_2\text{N}$  to be the ground state, switching the ordering of the  $1\pi_u$  and  $2\sigma_g$  orbitals. This suggested ground-state molecular orbital configuration has also been confirmed by Ornellas and Iwata.<sup>5</sup> The  $2\sigma_g$  and  $2\sigma_u$  orbitals arise from the symmetric and antisymmetric combinations of the (Si) valence shell electrons. The  $2\sigma_g$  and  $1\pi_u$  orbitals can lie especially close in energy after consideration of s–p hybridization is made and the  $1\pi_u$  orbital could easily be considered to lie higher in energy than the  $2\sigma_g$  orbital. This change would account for both the Brugh and Morse<sup>6</sup> MO configuration and the Goldberg<sup>4</sup> and Ornellas and Iwata<sup>5</sup> MO configuration (with the re-ordering of the  $1\pi_u$  and  $2\sigma_g$  orbitals) and suggests a much stronger interaction between the molecular orbitals on the end silicon atoms.

The modified molecular orbital diagram is also effective for explaining the observed Si–N bond length change<sup>6</sup> of only 0.0052 Å upon excitation of an electron from the  $2\sigma_u$  to the  $1\pi_g$  orbital. Because both of these orbitals are Si–N–Si nonbonding (and, nominally, Si–Si antibonding, with significant silicon–silicon interaction), promotion of an electron does not change the overall bond order of the molecule, and thus a small bond length change is accurately predicted.

**Ionization Potential of  $\text{Si}_2\text{N}$ .** While previous theory<sup>4,5</sup> predicts a highest occupied Si–N nonbonding  $1\pi_g$  molecular orbital, as suggested by Brugh and Morse,<sup>6</sup> it should be clear that these calculations indicate also a significant Si–Si interaction. Brugh and Morse, who established an upper bound of 8.51 eV for the  $\text{Si}_2\text{N}$  ionization potential, concluded<sup>6</sup> that the removal of an electron from this orbital corresponds essentially to the removal of an electron from a silicon 3p atomic orbital, and therefore that the IP of  $\text{Si}_2\text{N}$  would approximate that of atomic silicon ( $\approx 8.1$  eV<sup>7</sup>). However, our results indicate that the IP must be lower than 6.4 eV, in agreement with the suggestion of Goldberg et al.<sup>4</sup>

A more fundamental explanation of this discrepancy is that a single electron in the  $1\pi_g$  orbital (formed by a nominally antibonding combination of silicon 3p orbitals) does not bear close correspondence to a silicon “3p atomic orbital”. In other words, the electron occupying this orbital is not in one silicon 3p (atomic) orbital or the other (which would correspond to an IP of  $\sim 8.1$  eV), but rather in a molecular orbital which represents the combination of the two atomic silicon orbitals.<sup>31</sup> Since this molecular orbital is Si–Si antibonding, the nature of the orbital can result in the lowering of the energy required to remove an electron.

The effects of  $\text{Al}_2\text{O}$  (mass 70) on the nonresonant spectra observed in this study can again be considered. A large drop in the nonresonant signal intensity is observed between scans of energy greater than or equal to 8.5 eV and scans equal to or less than 7.9 eV for the mass 70 peak. This drop, which is seen for both  $\text{N}_2\text{O}$  and  $\text{NO}_2$  reactant modes is undoubtedly due to the fact that  $\text{Al}_2\text{O}$  is not ionized below 8.5 eV. We also note that the data in Figures 1–4 are consistent with the ionization potential of  $\text{Si}_2\text{C}$  which has been calculated<sup>10</sup> to be between 9.1 and 9.4 eV, and experimentally verified<sup>12</sup> at 9.1–9.2 eV. The presence of an  $\text{Si}_2\text{C}$  signal for the two-photon ArF and KrF ionization scans depicted in Figures 1 and 2 and the absence of the peak corresponding to this ion in Figures 3 and 4 is completely consistent with the  $\text{Si}_2\text{C}$  ionization potential. Unfortunately, the molecular orbital scheme which we have just

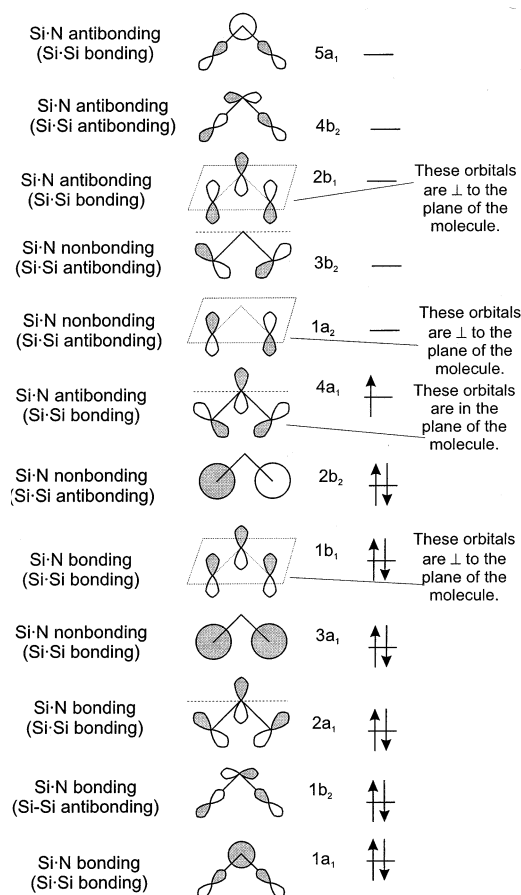


**Figure 6.** Molecular orbital correlation diagram for  $C_{2v}$  (bent) Si–N–Si ( $\text{BA}_2$ ) based on the configuration reported by Ornellas and Iwata.<sup>5</sup> The plane of the molecule is the  $y$ - $z$  plane.

considered for  $\text{Si}_2\text{N}$  must necessarily be modified to deal with  $\text{Si}_2\text{C}$ . Thus additional experimental and theoretical work on this molecule will be necessary.

**Cyclic ( $C_{2v}$ )  $\text{Si}_2\text{N}$  and  $\text{Si}_2\text{O}$ .** An alternate explanation for the observed upper bound on the ionization potential may be found in the analysis of the bent (cyclic) isomer of  $\text{Si}_2\text{N}$ . Ornellas and Iwata<sup>5</sup> confirmed that the bent (cyclic) symmetric isomer be observed in the gas phase, lying only  $\sim 4.90$  kcal/mol (0.2 eV) higher in energy than the linear symmetric isomer. The molecular orbital diagram constructed to be congruent to their molecular orbital designation, shown in Figure 6, is also appropriate for the ground-state cyclic isomer of  $\text{Si}_2\text{O}$ .

The highest occupied molecular orbital for the  $C_{2v}$  configuration is formed from a linear Si–N nonbonding orbital (Figure 5) that becomes more Si–N antibonding and strongly Si–Si bonding when bent. As the molecule is bent, the HOMO transforms from the  $1\pi_g$  orbital (localized on the end atoms) to the  $4a_1$  orbital (now involving the central nitrogen atom and therefore less localized on the end atoms) corresponding to the makeup of the cyclic isomer. Since the HOMO of the cyclic isomer is antibonding, it should be at least as easy to remove an electron as from the linear  $\text{Si}_2\text{N}$ , if not easier. Because the ground-state cyclic isomer of  $\text{Si}_2\text{O}$  is a fourteen valence electron molecule, the molecular orbital scheme of Figure 6, indeed, suggests that it will have a higher ionization potential than  $\text{Si}_2\text{N}$ .

**Acknowledgment.** A portion of this research was performed in the William R. Wiley Environmental Molecular Sciences Laboratory (EMSL) at the Pacific Northwest National Laboratory (PNNL). Operation of the EMSL is funded by the Office



of Biological and Environmental Research in the U.S. Department of Energy (DOE). PNNL is operated by Battelle for the U.S. DOE under Contract DE-AC06-76RLO 1830. K.A.P. was supported by the Division of Chemical Sciences in the Office of Basis Energy Sciences of the U.S. DOE.

## References and Notes

- (1) Zoethout, E.; Gurlu, O.; Zandvliet, H. J. W.; Poelsema, Bene. *Surf. Sci.* **2000**, *452*, 247. Winstead, C. B.; Paukstis, S. J.; Gole, J. L. *J. Mol. Spectrosc.* **1995**, *173*, 311. Cai, Z. L.; Martin, J. M. L.; Francois, J. P.; Gijbels, R. *Chem. Phys. Lett.* **1996**, *252*, 398, and references therein. Jungnickel, G.; Frauenheim, T.; Jackson, K. A. *J. Chem. Phys.* **2000**, *112* (3), 1295. Manson, E. L.; Clark, W. W.; DeLucia, F. C.; Gordy, W. *Phys. Rev. A* **1977**, *15* (1), 223. Lovas, F. J.; Maki, A. G.; Olson, W. B. *J. Mol. Spectrosc.* **1981**, *87* (2), 449. Botschwina, P.; Rosmus, P. *J. Chem. Phys.* **1985**, *82* (3), 1420.
- (2) Zmbov, K. F.; Margrave, J. L. *J. Am. Chem. Soc.* **1967**, *89*, 2492.
- (3) Iraqi, M.; Goldberg, N.; Schwartz, H. *J. Phys. Chem.* **1993**, *97*, 11371.
- (4) Goldberg, N.; Iraqi, M.; Schwarz, H.; Boldyrev, A.; Simons, J. *J. Chem. Phys.* **1994**, *101* (4), 2871.
- (5) Ornellas, F. R.; Iwata, S. *J. Phys. Chem.* **1996**, *100*, 10919.
- (6) Brugh, D. J.; Morse, M. D. *Chem. Phys. Lett.* **1997**, *267*, 370.
- (7) Moore, C. E. N. B. S. Circular No. 467 (U.S. GPO, Washington, DC 1971); Vol. 2.
- (8) DeKock, R. L.; Yates, B. F.; Schaefer, H. F. *Inorg. Chem.* **1989**, *28*, 1680.
- (9) Boldyrev, A. I.; Simons, J. *J. Phys. Chem.* **1993**, *97*, 5875.
- (10) Boldyrev, A. I.; Simons, J.; Zakrzewski, V. G.; vonNiessen, W. *J. Phys. Chem.* **1994**, *98*, 1427.
- (11) (a) Winstead, C. B. Laser Spectroscopy of Small Metal and Semiconductor Molecules. Ph.D. Thesis, Georgia Institute of Technology, (June 1995) 147; (b) Winstead, C. B.; Paukstis, S. J.; Walters, J. L.; Gole, J. L. *J. Chem. Phys.* **1995**, *102*, 1877.
- (12) Brugh, D. J. Ph.D. Thesis, The University of Utah, December 1997.
- (13) Atkins, P. *Physical Chemistry*, 5th ed.; W. H. Freeman, and Company: New York, 1994; C7.
- (14) Herzberg, Gerhard. *Molecular Spectra and Molecular Structure IV, Electronic Spectra and Electronic Structure of Polyatomic Molecules*; Van Nostrand Reinhold Co.: New York, 1966.
- (15) See also Gole, J. L.; Paukstis, S. J.; Dixon, D. A.; Peterson, K. A. Molecular Electronic Structure, Electronic Spectra, Ionization Potential, and Ground-State Spin-Orbit Splitting of Si<sub>2</sub>N. *J. Chem. Phys.*, submitted.
- (16) This also affects the intensity of the two-photon single color resonant Si<sub>2</sub>N electronic spectrum. See also ref 15, and Paukstis, S. J. Ph.D. Thesis, Georgia Institute of Technology, December 2000.
- (17) McQuaid, M. J.; Gole, J. L. *Chem. Phys.* **2000**, *260*, 867.
- (18) Bartlett, R. J.; *J. Phys. Chem.* **1989**, *93*, 1697. (b) Kucharski, S. A.; Bartlett, R. J. *Adv. Quantum Chem.* **1986**, *18*, 281. (c) Bartlett, R. J.; Stanton, J. F. In *Reviews of Computational Chemistry*; Lipkowitz, K. B., Boyd, D. B., Eds.; VCH Publishers: New York, 1995; Vol. 5, Chapter 2, p 65.
- (19) Hampel, C.; Peterson, K. A.; Werner, H.-J. *Chem. Phys. Lett.* **1990**, *190*, 1.; Deegan, M. J. O.; Knowles, P. J. *Chem. Phys. Lett.* **1994**, *227*, 321; Knowles, P. J.; Hampel, C.; Werner, H.-J. *J. Chem. Phys.* **1993**, *99*, 5219.
- (20) MOLPRO is a package of ab initio programs written by H.-J. Werner and P. J. Knowles with contributions from Almlöf, J.; Amos, R. D.; Berning, A.; Cooper, D. L.; Deegan, M. J. O.; Dobbyn, A. J.; Eckert, F.; Elbert, S. T.; Hampel, C.; Lindh, R.; Lloyd, A. W.; Meyer, W.; Mura, M. E.; Nicklass, A.; Peterson, K. A.; Pitzer, R. M.; Pulay, P.; Schütz, M.; Stoll, H.; Stone, A. J.; Taylor, P. R.; Thorsteinsson, T.
- (21) Dunning, T. H., Jr. *J. Chem. Phys.* **1989**, *90*, 1007; Kendall, R. A.; Dunning, T. H., Jr.; Harrison, R. J. *J. Chem. Phys.* **1992**, *96*, 6796; Woon, D. E.; Dunning, T. H., Jr. *J. Chem. Phys.* **1993**, *99*, 1914; Peterson, K. A.; Kendall, R. A.; Dunning, T. H., Jr. *J. Chem. Phys.* **1993**, *99*, 1930; Peterson, K. A.; Kendall, R. A.; Dunning, T. H., Jr. *J. Chem. Phys.* **1993**, *99*, 9790; Woon, D. E.; Dunning, T. H., Jr. *J. Chem. Phys.* **1995**, *103*, 4572.
- (22) (a) Dixon, D. A.; Feller, D.; Peterson, K. A. *J. Phys. Chem.* **1997**, *101*, 9405; (b) Peterson, K. A.; Xantheas, S. S.; Dixon, D. A.; Dunning, T. H., Jr. *J. Phys. Chem. A* **1998**, *102*, 2449. (c) Kumaran, S. S.; Su, M. C.; Lim, K. P.; Michael, J. V.; Klippenstein, S. J.; DeFelice, J.; Mudipalli, P. S.; Kiefer, J. H.; Dixon, D. A.; Peterson, K. A. *J. Phys. Chem.* **1997**, *101*, 8653. (d) Feller, D.; Dixon, D. A.; Peterson, K. A. *J. Phys. Chem. A* **1998**, *102*, 7053. (e) Feller, D.; Peterson, K. A. *J. Chem. Phys.* **1998**, *108*, 154. (f) Feller, D.; Peterson, K. A. *J. Chem. Phys.* **1999**, *110*, 8384. (g) Dixon, D. A.; Feller, D. *J. Phys. Chem. A* **1998**, *102*, 8209. (h) Dixon, D. A.; Feller, D. *J. Phys. Chem. A* **1999**, *103*, 4744. (i) Feller, D.; Dixon, D. A. *J. Phys. Chem. A* **1999**, *103*, 641. (j) Dixon, D. A.; Feller, D.; Peterson, K. A.; Gole, J. L. *J. Phys. Chem. A* **2000**, *104*, 232. (k) Feller, D.; Dixon, D. A. *J. Chem. Phys.* **2001**, *115*, 3484. (l) Ruscic, B.; Feller, D.; Dixon, D. A.; Peterson, K. A.; Harding, L. B.; Asher, R. L.; Wagner, A. F. *J. Phys. Chem. A* **2001**, *105*, 1. (m) Ruscic, B.; Wagner, A. F.; Harding, L. B.; Asher, R. L.; Feller, D.; Dixon, D. A.; Peterson, K. A.; Song, Y.; Qian, X.; Ng, C.; Liu, J.; Chen, W.; Schwenke, D. W. *J. Phys. Chem. A*, in press.
- (23) Peterson, K. A.; Woon, D. E.; Dunning, T. H., Jr. *J. Chem. Phys.* **1994**, *100*, 7410.
- (24) Peterson, K. A.; Dunning, T. H., Jr. To be published.
- (25) Davidson, E. R.; Ishikawa, Y.; Malli, G. L. *Chem. Phys. Lett.* **1981**, *84*, 226.
- (26) Drowart, J.; DeMaria, G.; Inghram, Mark G. *J. Chem. Phys.* **1958**, *29* (5), 1015–1021. Verhaegen, G.; Stafford, F. E.; Drowart, J. *J. Chem. Phys.* **1964**, *40* (6), 1622–1628.
- (27) Paukstis, S. J. Ph.D. Thesis, Georgia Institute of Technology, December 2000.
- (28) Ho, P.; Burns, R. P. *High Temp. Sci.* **1980**, *12*, 31.
- (29) (a) Masip, J.; Clotet, A.; Ricart, J. M.; Illas, F.; Rubio, J. *Chem. Phys. Lett.* **1988**, *144*, 4, 373–377. (b) Cai, Mingfang; Carter, Christopher C.; Miller, Terry A.; Bondybey, V. E. *J. Chem. Phys.* **1991**, *95*, 1, 73–79.
- (30) See ref 7, Volume 1.
- (31) When the example of atoms at the heart of the allyl radical (CH<sub>2</sub>CHCH<sub>2</sub>) are considered, it is found that the HOMO will be of <sup>1</sup>A<sub>g</sub> form, with outer-to-inner carbon of nonbonding character, and outer-to-outer carbons of antibonding character. Since Si and C are isovalent, if Morse's theory were correct, the allyl radical should have roughly the same ionization potential as the carbon atom (11.261).<sup>30</sup> However, the reported ionization potential of the allyl radical is 8.13 eV (Houle, F. A.; Beauchamp, J. A.; *J. Am. Chem. Soc.* **1978**, *100*, 3290), 73–79.